



Contents lists available at SciOpen

Food Science and Human Wellness

journal homepage: <https://www.sciopen.com/journal/2097-0765>

Lactiplantibacillus plantarum KX041 regulates lipid accumulation and intestinal flora to alleviate inflammatory obesity and its application in dairy products

Fangfang Yue^{1,2}, Haoyue Han^{1,2}, Jiaxin Xu^{1,2}, Beisenbayeva Kamila^{1,2}, Peiyao Yang^{1,2}, Yiming Zheng^{1,2}, Yulin Zhang^{1,2}, Xin Sun³, Fan Zhang^{1,2,*}, Xin Lü^{1,2,*}

¹ College of Food Science and Engineering, Northwest A&F University, Yangling 712100, Shaanxi, China

² Shaanxi Engineering Research Centre of Dairy Products Quality, Safety and Health, Yangling, Shaanxi, 712100, China

³ Xijing Hospital, the Fourth Military Medical University. No. 127, Changle West Road, Xi'an, Shaanxi, 710032, China.

ABSTRACT: *Lactobacillus* exhibits considerable potential in preventing metabolic disorders. The identification and characterization of novel *Lactobacillus* species hold significant practical value for the development of functional dairy products. *Lactiplantibacillus plantarum* KX041 is presumed to have potential probiotic functions due to its ability to produce functional extracellular polysaccharides. Therefore, this study aims to further investigate the effects and underlying mechanisms of both live and heat-inactivated *L. plantarum* KX041 on inflammatory obesity, and to preliminarily assess its application potential in dairy fermentation. *In vitro*, *L. plantarum* KX041 significantly inhibited adipocyte differentiation and reduced intracellular lipid accumulation, particularly at a concentration of 40%. The mechanism involved downregulating the mRNA expression of *CEBPA* and *Fabp4*. *In vivo*, activity and inactivated of *L. plantarum* KX041 can improve adipose accumulation (*FAS* and *FABP2*, *CEBPA*), intestinal barrier dysfunction (*Occludin*), systemic inflammation (*IL-6*) by regulating the transcription level of key genes. Additionally, *L. plantarum* KX041 improved inflammatory obesity by mitigating symptoms such as insulin resistance, liver dysfunction, and hyperlipidemia. Furthermore, 16S rRNA sequencing and correlation analysis suggested intestinal microbiota community structure is significantly associated with the levels of SCFAs. *L. plantarum* KX041 may enhance the production of acetic and butyric acids by promoting *Lactobacillus* colonization and reducing the abundance of *Ruminiclostridium_9*. Finally, based on its favorable functional properties and fermentation performance, *L. plantarum* KX041 shows promise as a candidate single-strain starter culture for the development of functional dairy products.

Key words: *Lactiplantibacillus plantarum* KX041; probiotics; Inflammatory obesity; Gut microbiota; functional dairy products

1. Introduction

The increasing number of overweight and obese people worldwide has become a growing public health problem [1]. Obesity often leads to systemic low-grade inflammation and associates with an increased risk of numerous chronic diseases [2], such as cancer, cardiovascular disease, etc [3]. Genetic and environmental factors are the main causes of obesity [4]. High fiber diet (HFD) can cause an imbalance between energy

*Corresponding author
xinlu@nwsuaf.edu.cn

Received 11 September 2025
Received in revised from 14 October 2025
Accepted 11 December 2025

intake and consumption, resulting in energy and fat accumulation in the body, which is usually accompanied by metabolic disorders and intestinal microbiota disorders [5]. It has been reported that HFD can cause insulin resistance in the body and affect the composition of gut microbes to regulate fat metabolism [6]. Therefore, altering the microbiota composition is expected to be a potential strategy for relieving obesity.

It has been reported that specific bacterial strains *K. kefirifaciens* M1 and *L. mali* APS1 isolated from Kefir have been shown to be able to improve obesity by regulating the tripartite relationship between host, microbiome and metabolites [7]. They have been found to manipulate different abundances of gut flora to regulate metabolite expression, ultimately affecting fat accumulation and inflammation in obese individuals. In addition, three strains of *Lactobacillus* were screened from feces and proved to be able to alleviate obesity syndrome by inhibiting the intake of carbohydrates and excessive absorption of lipids *in vitro* [8]. *L. fermentum* SMFM2017-4, screened from Kimchi, inhibited glucosidase and pancreatic lipase activities and 3T3-L1 preadipocyte differentiation, down-regulated *Fas* expression and up-regulated *GPx-1* expression, and decreased serum TG, adipocyte size and liver steatosis [9]. Therefore, probiotics, especially *Lactobacillus*, have potential value in alleviating obesity.

In this preliminary study, a strain of *L. plantarum* KX041 capable of producing exopolysaccharides (EPS) was isolated from traditional Chinese pickled vegetables. Prior studies confirmed that EPS alleviates inflammatory obesity [10], although the anti-obesity mechanism of the *L. plantarum* KX041 strain itself remains unclear. Moreover, the synergistic effect of probiotics and prebiotics significantly enhances the production of short-chain fatty acids (SCFAs), establishing it as a novel strategy for microbiota-targeted intervention in obesity [11]. Consequently, intervention with *L. plantarum* KX041—a strain capable of producing prebiotic EPS may exert greater potential in alleviating obesity in mice. In addition, studies have shown that paraprobiotic intervention (inactivated microbial cells or cell components that provide health benefits) is more suitable than direct probiotic intervention. For example, *Lactobacillus plantarum* L67 probiotics and paraprobiotics were found can reduce the symptoms of colitis by inhibiting DSS induced pro-inflammatory factors, and paraprobiotics are safer and more stable [12]. However, since the live *L. plantarum* KX041 can produce prebiotic EPS, it remains to be further studied whether the combined effect is stronger than that of the heat-killed *L. plantarum* KX041 (paraprobiotics). Finally, the application of functional probiotics in dairy products is the key to determine their actual value, and good curd characteristics and flavor will be beneficial to the development of functional probiotics products.

In this study, live and heat-killed *L. plantarum* KX041 were used to intervene in high-fat diet-induced obesity in mice, exploring their regulatory effects on inflammation, metabolism, and intestinal microbial disorders. Additionally, *L. plantarum* KX041 was fermented in milk to investigate its fermentation characteristics and flavor, providing theoretical support for the development of functional yogurts that can alleviate obesity.

2. Materials and methods

2.1 Materials

The strain *L. Plantarum* KX041 (GenBank No. MW468093) was isolated and screened by our laboratory from Chinese traditional pickle juice from Kaixian County, Chongqing, and stored at -80°C ; Commercial bacteria yogurt fermentation powder (Beijing Chuanxiu Technology Co., LTD); Oral glucose solution (Aonu Pharmaceutical Co., Ltd.); Insulin injection (Novo Nordisk Pharmaceuticals Co., Ltd.); Hematoxylin and eosin (H&E) staining solution (Shaanxi Zhonghui Hecai Biomedical Technology Co., Ltd.); Short-chain fatty acid standards (Sigma-Aldrich); Xylene (analytical grade, Chengdu Kelong Chemical Co., Ltd.); ELISA kits (Beijing Sinobiological Co., Ltd.): TNF- α , IL-1 β , and IL-6.

2.2 Preparation of live and heat-killed *L. Plantarum* KX041 suspension, and bacterial cellular contents

L. Plantarum KX041 was inoculated on Modified MRS liquid medium [13] at 3% and cultured at 37°C for 16 h. After centrifugation at 6000 g for 20 min, collect the bacterial sediment. Wash the bacteria with physiological saline three times (6000 g, 20 min) and concentrate to a bacterial concentration of approximately 1×10^9 CFU/mL to obtain live *L. plantarum* KX041 suspension. Heat-inactivated *L. plantarum* KX041 suspension was obtained by heating the 100°C for 30 min.

L. plantarum KX041 was consecutively activated twice in Modified MRS broth at 37°C for 18 h per cycle to ensure metabolic activity. 3% (v/v) inoculum was transferred to fresh Modified MRS broth and incubated at 37°C for 28 h ($\text{OD}_{600} \approx 6.0$). Cells were pelleted by centrifugation at $6,000 \times \text{g}$ for 20 min, with complete supernatant removal. The bacterial pellet was washed thrice with phosphate-buffered saline (PBS, pH 7.4; Solarbio) under identical centrifugation conditions. Washed cells were resuspended in PBS at 1/20 of the original culture volume, achieving a final concentration of $\sim 1 \times 10^9$ CFU/mL. Using a probe ultrasonic instrument (Scientz-IID, 6mm probe), perform cell lysis in an ice bath ($\leq 4^{\circ}\text{C}$) to obtain cellular content. The process employs a pulse mode with 150W output power, a 3s on/off duty cycle, and a 20 min duration.

2.3 Induction and treatment of Preadipocytes 3T3-L1

The 3T3-L1 preadipocyte cell line were divided into Untreated control group (CK, undifferentiated state), differentiation control group (0, standard induction protocol) and experimental intervention groups with varying concentrations of test compounds (parallel interventions with 10%, 20%, 40%, and 60% bacterial lysate incorporated into induction medium). All cellular populations were maintained in Dulbecco's Modified Eagle Medium (DMEM) supplemented with 10% fetal bovine serum (FBS) and 1% penicillin/streptomycin antibiotic cocktail (v/v), under standardized culture conditions (37°C , 5% CO_2 humidified atmosphere) until contact inhibition. Inducer A (a differentiation DMEM mixture containing 10% fetal bovine serum, $1 \mu\text{M}$ dexamethasone, 0.5 mM methylisobutylxanthine, and $1 \mu\text{g}/\text{mL}$ insulin) and Inducer B (a differentiation medium consisting of DMEM spiked with 10% fetal bovine serum and $1 \mu\text{g}/\text{mL}$ insulin) were used to intervene the cells at different times, and the pre-fat cells were finally successfully differentiated into lipid droplets. The specific induction process was referred to the composition of previous studies [10].

2.4 HFD Animal model

44 SPF male C57BL/6J mice (7-week-old) were purchased from Hunan Slyke Jingda Experimental Animal Co., LTD. (Hunan, China). All mice were cared in accordance with the guidelines for the Care and Use of Laboratory Animals recommended by the National Institutes of Health, and the experimental program was approved by the Animal Experimental Ethics Committee of Xi'an Jiaotong University (Permission No. SCXK 2021-006). The mice were placed in an independent space with $20\pm 2^{\circ}\text{C}$, $55\%\pm 5\%$ relative humidity and alternating light/darkness for 12 h. Experimental diets comprising a 60% high-fat formulation (TP2330055A) and corresponding low-fat control (TP2330055AC) were procured from Nantong Telophi Feed Technology Co., Ltd., with subsequent sterilization conducted through cobalt-60 γ -ray irradiation. After a period of acclimation, the mice were randomly divided into four groups: CK with normal chow diet ($n = 10$), HFD with high fat diet ($n = 12$), HKLP with HFD and daily oral gavage heat-killed *L. Plantarum* KX041 ($n = 10$) and LP with HFD and daily oral gavage living *L. Plantarum* KX041 ($n = 12$) for 10 weeks. After fasting for 12 h, following isoflurane-induced anesthesia, the mice were humanely sacrificed through rapid cervical dislocation protocol. Intestinal tissue from the cecum to the anus and blood samples was collected and the length of the colon was measured. The weight changes of mice were record , and the tissue (fat, liver, kidneys and spleen) was taken out and weighed and frozen at -80°C . Fresh livers were soaked in 4% polyformaldehyde for 24 h, then embedded in paraffin and cut into $5\ \mu\text{m}$ sections. After treatment with xylene and ethanol of varying concentrations, the sections were stained with hematoxylin and eosin (H&E) and observed under a fluorescence microscope.

2.5 Blood biochemical index test

At the conclusion of the 9-week intervention period, glucose homeostasis was evaluated through an oral glucose tolerance test (OGTT). Following a 16-hour fasting protocol, mice received an oral gavage of glucose solution (2 g/kg body weight). Serial blood glucose measurements were obtained via tail vein sampling at baseline (0 min) and subsequent timepoints (15, 30, 60, 120 min) using a standardized glucometer.

After a 3-day recovery interval, insulin sensitivity was assessed via insulin tolerance testing (ITT). Subjects underwent 4 h of fasting prior to intraperitoneal administration of insulin (0.75 U/kg body weight). Capillary blood glucose levels were monitored at 15-minute intervals (0, 15, 30, 45, 60 min) post-injection through sequential tail-tip blood collection.

Serum concentrations of lipid parameters including total cholesterol (TC), triglycerides (TG), high/low-density lipoprotein cholesterol (H/LDL-C), along with hepatic enzymes alanine transaminase (ALT) and aspartate transaminase (AST), were quantitatively assessed using an automated biochemical analyzer. In parallel, serum concentrations of pro-inflammatory mediators - tumor necrosis factor-alpha (TNF- α), interleukin-1 beta (IL-1 β), and interleukin-6 (IL-6) were determined through enzyme-linked immunosorbent assay (ELISA) following standardized manufacturer protocols (Shanghai Xinle Biotechnology Co., LTD).

2.6 Quantification of gene expression in liver and colon

Total RNA was isolated using TRIzol reagent through a standard phenol-chloroform extraction protocol. First-strand cDNA synthesis was performed using the PrimeScript RT reagent Kit. Quantitative PCR analysis

was carried out in triplicate using SYBR Green qPCR Master Mix on a CFX96 Touch™ Real-Time PCR system. The thermal cycling protocol consisted of initial denaturation at 95°C for 30s, followed by 40 cycles of 95°C for 5 s and 60°C for 30 s. Target gene expression levels were normalized against the endogenous control *GAPDH*, with relative quantification calculated using the comparative $2^{-\Delta\Delta CT}$ method.

2.7 Analysis of gut microbiota and SCFAs

Total genomic DNA was isolated from fecal specimens employing the PowerSoil DNA isolation kit (MOBIO Laboratories). Purified DNA samples underwent bacterial rRNA gene amplification and paired-end sequencing (2×250 bp) on the Illumina HiSeq 2500 platform. Raw sequencing data were preprocessed through the QIIME pipeline (version 1.9.1) to generate high-quality reads. Subsequent bioinformatic processing involved three critical steps: (1) read merging using FLASH v1.2.7 with default parameters, (2) chimera detection and removal through UCHIME v4.2, and (3) operational taxonomic unit (OTU) clustering at 97% sequence similarity threshold via USEARCH v10.0. Taxonomic classification was performed using the Ribosomal Database Project (RDP) Classifier v2.2 with genus level resolution. Microbial diversity analysis included calculation of α -diversity indices (ACE, Chao1, Simpson, and Shannon) using Mothur software (v1.39.5). Beta diversity comparisons between sample groups were conducted through weighted UniFrac distance-based principal coordinate analysis (PCoA).

The content of SCFAs in feces was determined by gas chromatography. Approximately 200 mg of homogenized fecal specimens were suspended in 1.5 mL of ultrapure water and subjected to primary centrifugation (4°C, 12,000 × g, 10 min). The resultant supernatant underwent dual-stage filtration through 0.22 μ m organic nylon membranes, with the initial aqueous phase collected for subsequent acidification using 50% sulfuric acid (v/v). Following vortex agitation (5 min), the acidified mixture underwent liquid-liquid extraction with 0.8 mL diethyl ether through phase separation (30 min static incubation) and secondary centrifugation under identical parameters. Chromatographic separation was achieved using an RTX-WAX capillary column (30 m×0.25 m×0.25 m) coupled to flame ionization detection. The optimized thermal gradient protocol initiated at 50°C (1 min isothermal), followed by programmed increases: 15°C/min to 120°C, 5°C/min to 170°C, and final ramping at 15°C/min to 240°C (3 min hold). Carrier gas flow was maintained at 1.0 mL/min with splitless injection (1 μ L volume).

2.8 Application of *L. Plantarum* KX041 fermented dairy products

Fresh bovine milk (whole milk with 3.3% fat content and 3% protein content) was supplemented with 3%, 5%, 7% (w/v) sucrose and homogenized until complete dissolution. Prior to use, the fermentation vessel and associated sealing components underwent thermal sterilization through immersion in a boiling water bath (100°C) for 10 min. Then 80 mL of the prepared sucrose-milk solution was aseptically transferred into the pre-treated vessel, which was subsequently sealed and subjected to thermal conditioning in a water bath maintained at 60°C for 30 min, and cooled to ambient temperature. *L. Plantarum* KX041 was pre-cultured in MRS broth medium under standard conditions (37°C, 24 h). Cellular biomass was harvested through centrifugation at 8,000 × g for 10 min (4°C). The resultant cell pellet underwent two successive washing

cycles using sterile physiological saline (0.85% NaCl). Washed cells were resuspended in sterile saline at a standardized concentration of 100 mg wet weight/mL.

The prepared inoculum was aseptically introduced into the sterilized sucrose-milk matrix at 3% (v/v) inoculation ratio. Biological incubation proceeded in a temperature-regulated environment ($37^{\circ}\text{C} \pm 0.5^{\circ}\text{C}$) for 48 h under static conditions. Parallel experiments were conducted with commercial reference strains following identical procedural parameters. After fermentation, the fermented milk was placed in 4°C for ripening for 10 h. The pH of fermented milk was measured at 0 h, 2 h, 4 h, 6 h, 12 h, 24 h, 36 h and 48 h.

2.9 Sensory evaluation of dairy products

The sensory evaluation was conducted in accordance with the standardized triangle testing methodology specified in China's National Food Safety Standard for Fermented Milk (GB 19302-2010). Fourteen adult panelists (7 males and 7 females) with verified sensory acuity were systematically recruited following the standard's sample size requirements. All participants undergoing pre-test calibration exercises to ensure consistent evaluation criteria. The indicators and scoring criteria: Offensive Odor (scoring from 0 to 10 based on intensity of unpleasant smell); Acidity (scoring from 0 to 10 based on acidity level); Organization Status (scoring from 0 to 10 based on texture fineness and uniformity); Color (scoring from 0 to 10 based on uniformity of coloration); Milky Flavor (scoring from 0 to 10 based on sweetness and creamy aroma of milk).

2.10 Electronic nose and tongue detect the flavor of dairy products

Under room temperature conditions (25°C), the olfactory characteristics of fermented milk were collected using a PEN3-Plus electronic nose (Airsense Company, Schwerin, Germany). 5 mL fermented milk sample was placed in a sample vial, and headspace sampling was performed with the PEN3-Plus electronic nose. The procedure involved: 100 s of sensor cleaning; Inserting the sampling needle and pressure stabilization needle into the headspace of the vial; Extracting volatile compounds for 90 s, with stable values (typically recorded between 70–90 s) used for data analysis.

The fermented milk was filtered through double-layered degreased gauze to remove insoluble substances, then diluted fourfold with ultrapure water. Under room temperature conditions (25°C), an electronic tongue (Insent Company, Japan) was used to collect eight taste profile indicators: sourness, bitterness, astringency, bitterness aftertaste, astringency aftertaste, umami, umami aftertaste, and saltiness.

2.11 Statistical analysis

Statistical analyses were conducted using GraphPad Prism software (version 8.3.0.538). Group comparisons were performed through one-way analysis of variance (ANOVA) followed by Fisher's least significant difference (LSD) post-hoc test for multiple comparisons. Continuous variables are presented as mean \pm standard error of the mean (SEM), with P -values < 0.05 considered statistically significant. Pearson correlation coefficients quantifying associations between gut microbiota composition and SCFAs were calculated using R statistical environment (version 4.1.0).

3. Results and discussion

3.1 Effects of *L. Plantarum* KX041 cellular contents on Preadipocytes 3T3-L1

3T3-L1 preadipocytes exhibit the capacity for directed differentiation into adipocytes, enabling triglyceride accumulation and the formation of cells morphologically and functionally similar to mature white adipocytes [14]. Therefore, 3T3-L1 is an important *in vitro* model for obesity research. Through cytotoxicity test, it was found that the contents of *L. Plantarum* KX041 at 10-40% concentration had no significant effect on the survival rate of 3T3-L1 preadipocytes. While the contents of *L. Plantarum* KX041 at 60% and 80% concentration significantly reduced the survival rate of 3T3-L1 preadipocytes, especially at 80% concentration. Therefore, three concentrations of 10%, 20% and 40% were selected for the subsequent experiments (Figure 1A). The uninduced 3T3-L1 preadipocytes were triangular or polygonal, and the cells gradually became round after induction, and lipid droplets were formed in the cytoplasm. The effects of different concentrations of *L. Plantarum* KX041 bacterial contents on the differentiation of 3T3-L1 preadipocytes into lipid droplets were investigated by oil red O staining oil. The results showed that interventions with 10% *L. Plantarum* KX041 bacterial contents did not exhibit significant inhibitory effects. However, at the 20%, 40% and 60% concentration level, the intervention led to a reduction in both the number and size of lipid droplets (Figure 1B), indicating its role in decreasing cytoplasmic lipid accumulation during the differentiation of preadipocytes into mature cells.

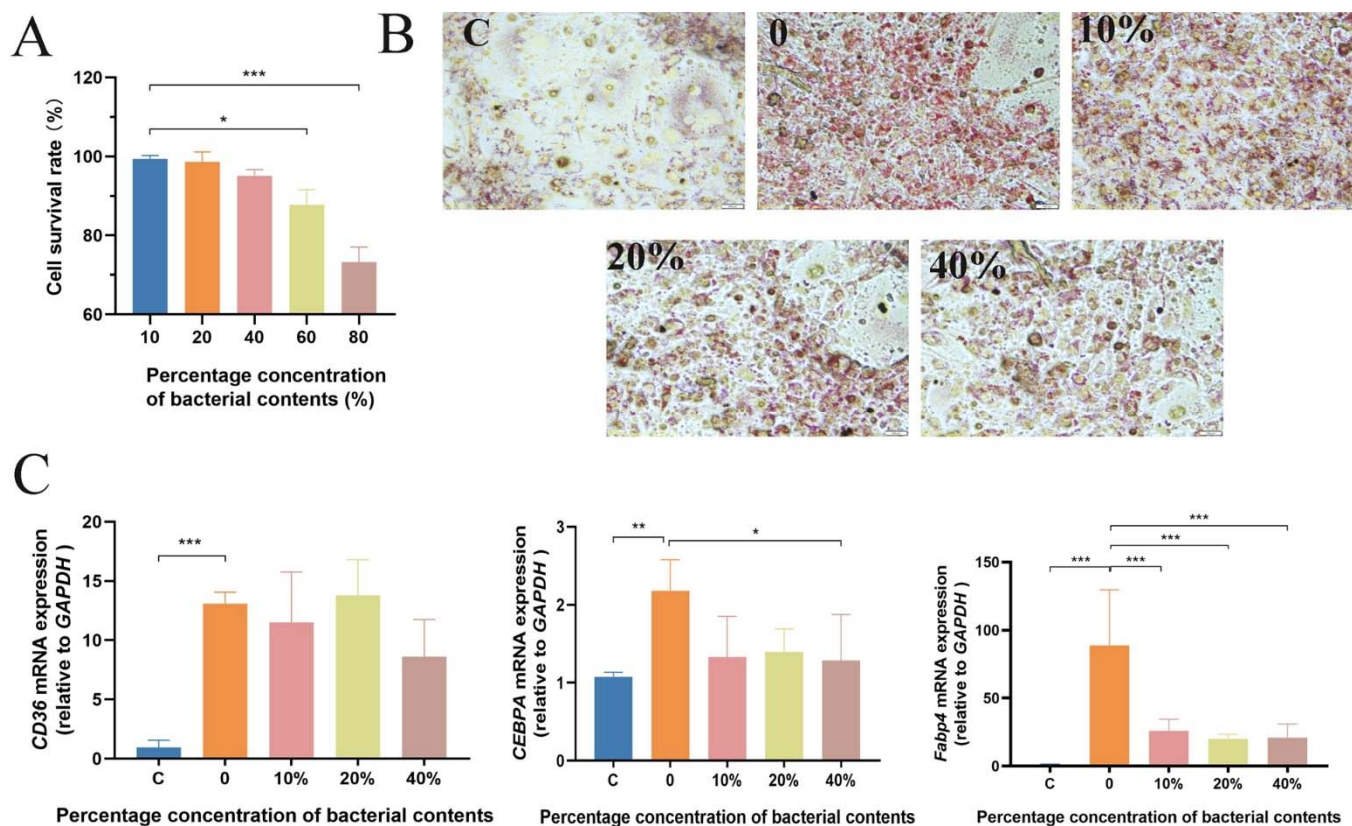


Figure 1 Effects of different concentrations of *L. plantarum* KX041 on 3T3-L1 preadipocytes in vitro. (A) The survival rate of 3T3-L1, (B) 3T3-L1 preadipocytes into lipid droplets (Oil red O staining, scale 100 μ m); (C) Transcript levels of genes involved in lipid anabolism: *CD36*, *CEBP*, *Fabp4*. *, **, *** represent $P < 0.05$, 0.01 and 0.001, respectively.

In normal adipocytes, lipid synthesis and degradation maintain a dynamic balance. Any imbalance in these processes may lead to related diseases [15]. During adipocyte differentiation, the sequential activation of transcription factors is tightly regulated. CD36, functioning as a transporter, mediates the uptake of oxidized low-density lipoprotein (ox-LDL) and long-chain fatty acids (LCFAs), playing a critical role in cellular lipid metabolism [16]. CCAAT/enhancer-binding protein alpha (CEBPA) promotes the differentiation of preadipocytes into mature adipocytes [17]; Fabp4 (Fatty Acid-Binding Protein 4) is a lipid-binding protein that plays a pivotal role in intracellular fatty acid transport and metabolism [18]. In this study, 3T3-L1 preadipocytes were treated with *L. plantarum* KX041 lysate for 8 days under differentiation induction. The results demonstrated that the bacterial lysate (particularly at 40% concentration) significantly suppressed adipocyte differentiation by downregulating mRNA expression of *CEBPA* and *Fabp4* (Figure 1C), thereby inhibiting lipid accumulation in adipocytes and the maturation of preadipocytes. However, no significant reduction was observed in *CD36* expression.

3.2 *L. Plantarum* KX041 improve the basic indicators of obese mice

The body weight of mice fed a high-fat diet (HFD, HKLP, and LP groups) was significantly higher compared to those fed a low-fat diet (CK group). Oral administration of both live and inactivated *L. Plantarum* KX041 significantly ameliorated body weight gain in mice (Figure 2A and B). Studies have found that obesity often leads to visceral organ pathologies, such as fatty liver disease and shortened colon length [19]. In this study, the HFD mice exhibited significantly higher liver, kidney, spleen, and epididymal fat weights compared to CK group (Figure 2E). The abnormalities in immune organ weights indirectly reflect systemic inflammatory responses. Notably, *L. plantarum* KX041 treatment markedly ameliorated these effects, with no statistically significant difference observed between live and inactivated bacterial intervention groups ($P > 0.05$). In addition, compared to CK group, HFD group exhibited a significantly shorter average colon length (Figure 2F). Live bacterial intervention attenuated this high-fat diet-induced colon shortening. Additionally, HFD mice showed markedly greater abdominal fat accumulation than CK group, whereas both live and inactivated bacterial treatments substantially reduced this effect. Excessive accumulation of white adipose tissue is a key factor affecting obesity, and its main role is to store energy and triglycerides (TG) [20]. After 10 weeks of HFD feeding, mice exhibited significantly larger average white adipose tissue (WAT) volume compared to those fed a normal diet. Relative to the CK group, HFD group showed looser, softer, and more fluid epididymal fat structure (Figure 2G), with markedly increased epididymal and subcutaneous fat mass (Figure 2F). *L. plantarum* KX041 intervention significantly reduced both epididymal and subcutaneous fat weight in obese mice, particularly subcutaneous fat. Notably, no statistically significant difference was observed between live and inactivated *L. plantarum* KX041 treatments in suppressing WAT accumulation. In addition, HE staining of liver tissue shows compared with the CK group, HFD mice exhibited increased hepatocyte volume, prominent intracytoplasmic lipid droplet vacuolation, and disorganized hepatic cord architecture, indicative of lipid accumulation and mild hepatic tissue injury. Following intervention with both inactivated and activated *L. Plantarum* KX041, hepatocyte morphology was largely restored to normal, vacuolation was reduced, and the hepatic cord structure showed substantial recovery (Supplementary Figure

1). These results demonstrate that *L. plantarum* KX041 ameliorates obesity in mice by reducing visceral organ and adipose tissue weight.

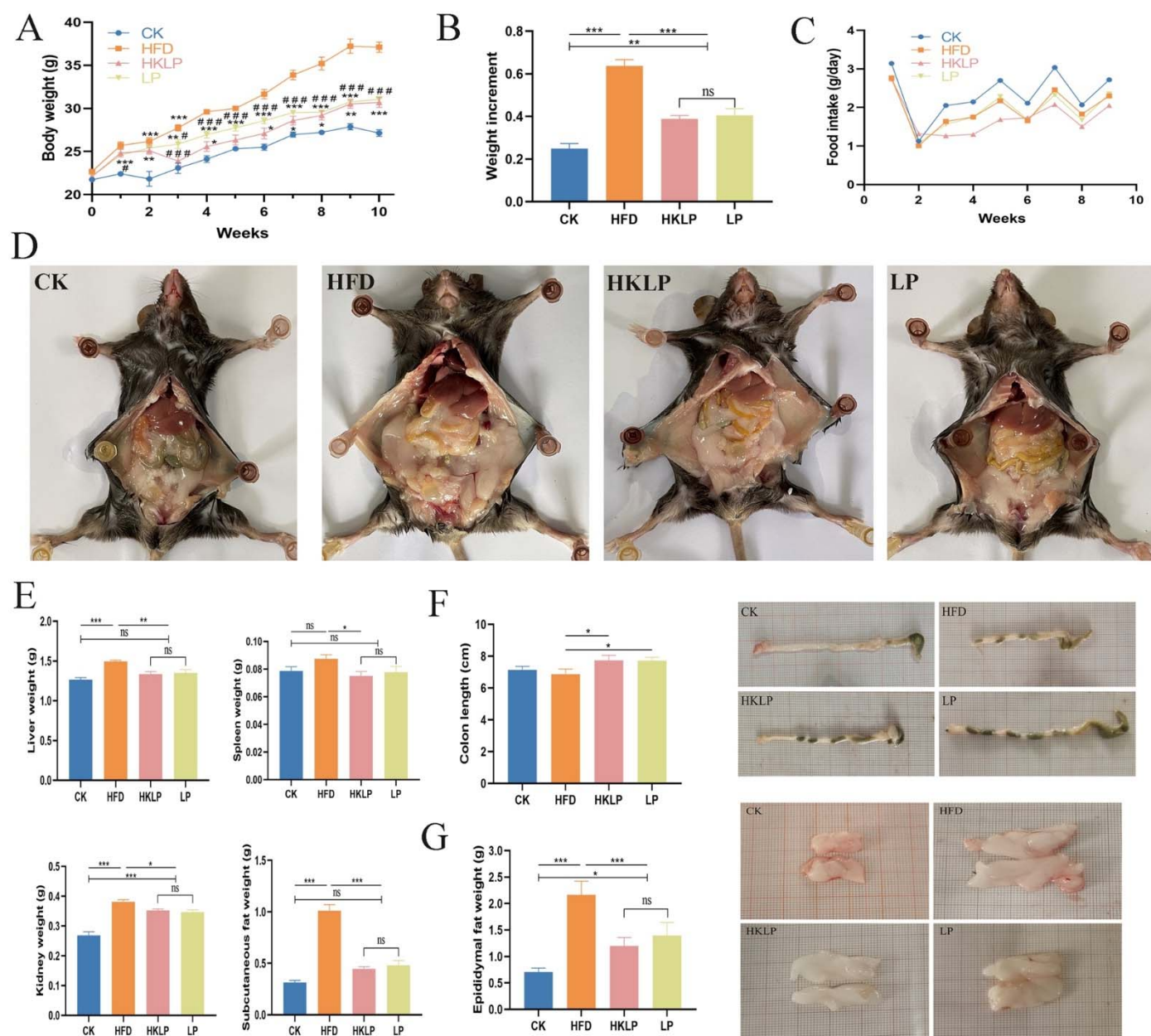


Figure 2 Effect of *L. plantarum* KX041 on inflammatory obesity-related indicators in HFD mice. (A) Body weight; (B) weight Gain; (C) food intake; (D) mouse abdominal cavity photograph; (E) live weight, spleen weigh, Kidney weight, subcutaneous fat; (F) colon length; (G) epididymal fat. *, **, *** represent $P < 0.05$, 0.01 and 0.001, respectively, while ns indicates no statistical difference.

3.3 *L. Plantarum* KX041 improved biochemical indexes of blood in obese mice

HFD typically impairs blood glucose levels and insulin [21]. Blood glucose homeostasis was assessed by measuring blood glucose levels before and after oral glucose (i.e., glucose tolerance test OGTT); while insulin sensitivity was assessed by measuring blood glucose levels before and after insulin injection (Insulin tolerance test, ITT). The OGTT (Figure 3A-a) and ITT (Figure 3B-a) tests revealed that compared to the normal diet group, HFD significantly elevated fasting blood glucose levels, while microbial intervention attenuated this increase. Besides, HFD group exhibited impaired glucose tolerance versus the CK group, with the highest area

under the curve (AUC). Both live and inactivated *L. plantarum* KX041 supplementation reduced AUC (Figures 3A-b and c). Meanwhile, the HFD group experienced the slowest rate of blood glucose reduction after insulin injection, indicating severe insulin resistance (Figures 3B-b). During 60–90 min (Figures 3B-c), the HKLP and LP groups showed significantly higher average blood glucose recovery than the HFD group ($P < 0.05$), demonstrating probiotic-induced improvement in insulin sensitivity and glycemic recovery.

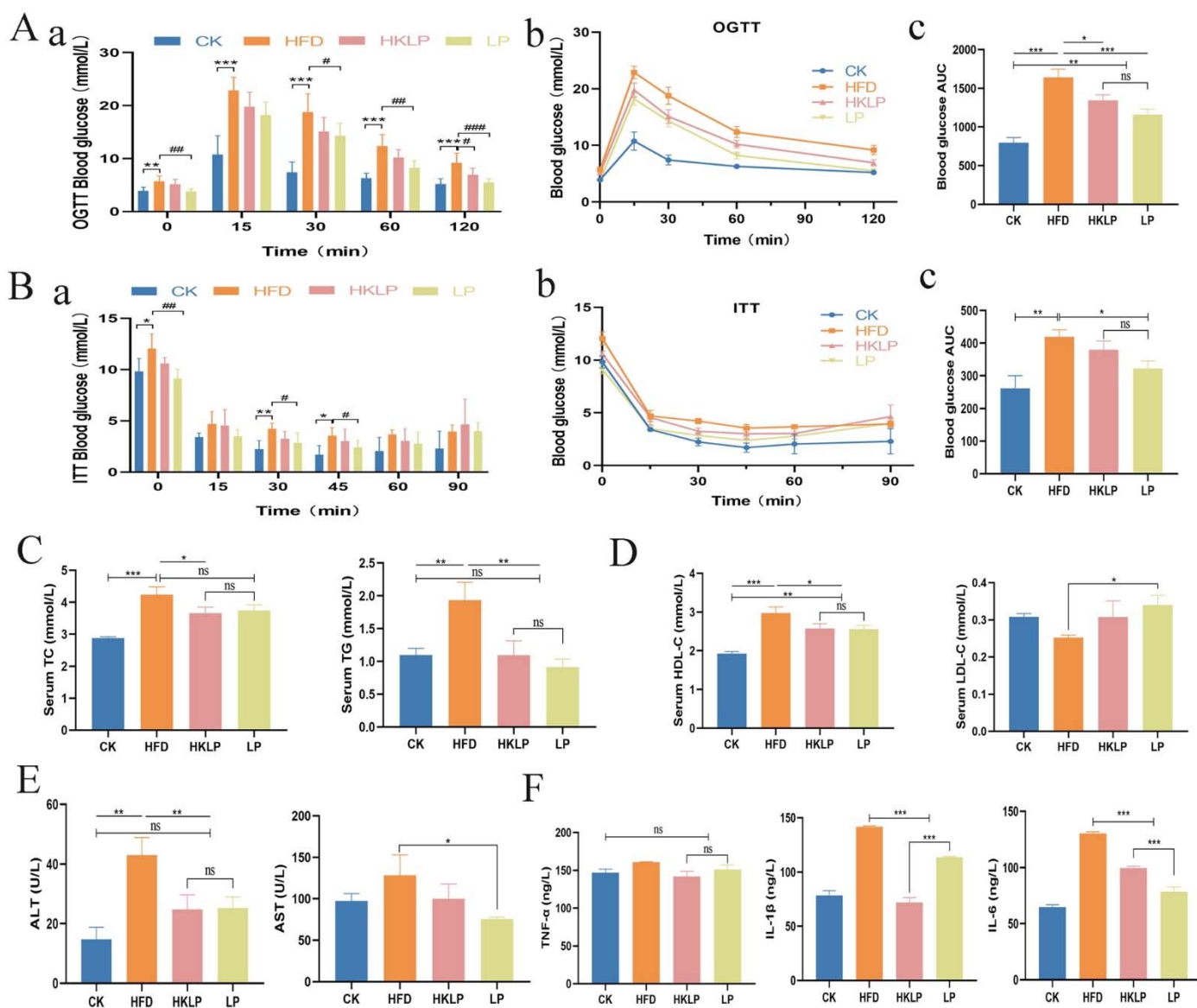


Figure 3 Effect of *L. plantarum* KX041 on blood biochemical indicators. (A) OGTT blood glucose (a), curve (b) and area under the curve (c); (B) ITT blood glucose (a), curve (b) and area under the curve (c); (C) blood fat: serum TC, Serum TG, (D) Serum HDL-c, serum LDL-c; (E) Indicators of liver function injury: ALT, AST; (F) content of serum inflammatory factors: IL-6, IL-1 β , TNF- α . * indicates HFD comparison with CK group, # indicates intervention group comparison with HFD group. In Figure A and B, * and #, ** and ##, *** and ### represent $P < 0.05$, 0.01 and 0.001, respectively, while ns indicates no statistical difference.

Serum TC, TG, HDL-c, and LDL-c are key biomarkers for assessing HFD-induced dyslipidemia [22]. The HFD significantly elevated serum TC, TG, and HDL-c levels while reducing LDL-c in mice. *L. plantarum* KX041 intervention markedly suppressed the increase in serum TG and HDL-c (Figures 3C and 3D), even restoring average TG levels to those of normal-weight mice. These results demonstrate its potent

ameliorative effects on obesity-associated dyslipidemia. Heat-inactivated *L. plantarum* KX041 significantly reduced serum TC levels, whereas live bacterial intervention notably suppressed the decrease in serum LDL-c.

ALT and AST levels serve as biomarkers for assessing liver function impairment [23]. Compared to the CK group, HFD mice exhibited significantly elevated serum ALT levels. Both HKLP (heat-killed KX041) and LP (live KX041) interventions markedly lowered ALT levels, with no statistically significant difference. Furthermore, LP group intervention attenuated the HFD-induced increase in serum AST (Figure 3E), while the HKLP group showed no significant effect. These differential effects likely stem from variations in their biological properties, metabolic outputs, and host interaction mechanisms. Studies have demonstrated that live bacteria, owing to their fully functional metabolic activities, can mitigate obesity by modulating host metabolism. For instance, *Bifidobacterium breve* improves liver function in overweight or obese individuals by regulating key serum metabolites and thereby affecting AST levels [24]. Although inactivated bacteria lack metabolic viability, they retain structural components such as membrane proteins. Notably, Amuc_1100, a protein derived from inactivated *Akkermansia muciniphila*, has been found to exert various immunometabolic effects by activating specific signaling pathways [25]. Research has established that chronic low-grade inflammation is closely linked to obesity and metabolic disorders. Inflammatory programs are activated during the early stages of adipose tissue expansion and further evolve during chronic obesity, driving the immune system toward a pro-inflammatory phenotype [26].

It was found that in obese mice, the levels of pro-inflammatory factors such as IL-6, IL-1 β and TNF- α secreted by adipocytes were key to assessing low inflammation [27]. Serum analysis of three pro-inflammatory factors (IL-6, IL-1 β , and TNF- α) revealed that the model group exhibited significantly higher levels of IL-6 and IL-1 β compared to the CK group. Both HKLP and LP interventions markedly suppressed serum IL-6 and IL-1 β levels, but showed no significant effect on TNF- α (Figure 3F). Research has confirmed that chronic inflammation plays a positive role in pathological obesity-induced insulin resistance, and that obesity-associated insulin resistance can trigger chronic inflammation in adipose tissue [28]. In this study, we further demonstrate that *L. plantarum* KX041 enhances insulin sensitivity and stabilizes glycemic control during its attenuation of systemic inflammation, ultimately contributing to obesity mitigation.

3.4 The effects of *L. plantarum* KX041 on transcriptional levels of specific genes

Analysis of mRNA transcriptional levels in liver tissue revealed that HFD group exhibited significant upregulation of genes (*FABP2*, *SREBP-1c*, *CEBPA*, *PPAR γ*) involved in adipocyte differentiation and lipogenesis compared to the control group (Figure 4A). Among these, *SREBP-1c* and *PPAR γ* are key hepatic genes regulating fatty acid synthesis and lipid accumulation. Their overexpression may upregulate downstream targets (e.g., *FAS*), which is a key limiting enzyme in fat synthesis [29]. *CEBPA* plays a critical role in promoting early adipocyte differentiation and maintaining the mature state of adipocytes. Research has found that *CEBPA* upregulation could drive the process of adipocyte differentiation, thereby promoting the occurrence and development of obesity-related diseases [30]. *FABP2* is an important fatty acid binding protein, and its abnormal expression is closely related to obesity, type 2 diabetes and cardiovascular disease

[31]. The study found that both heat-inactivated and live *L. plantarum* KX041 interventions significantly reduced *FAS* and *FABP2* levels. This suggests that both heat-inactivated and live *L. plantarum* KX041 suppress fat accumulation through a dual mechanism involving inhibition of both synthesis and absorption [32], which may be effective in preventing and treating obesity and related metabolic disorders. Furthermore, live *L. plantarum* KX041 significantly reduced the high expression of *CEBPA* mRNA caused by HFD, this suggests that it may block the maturation process of adipocytes, reducing excessive expansion of adipose tissue.

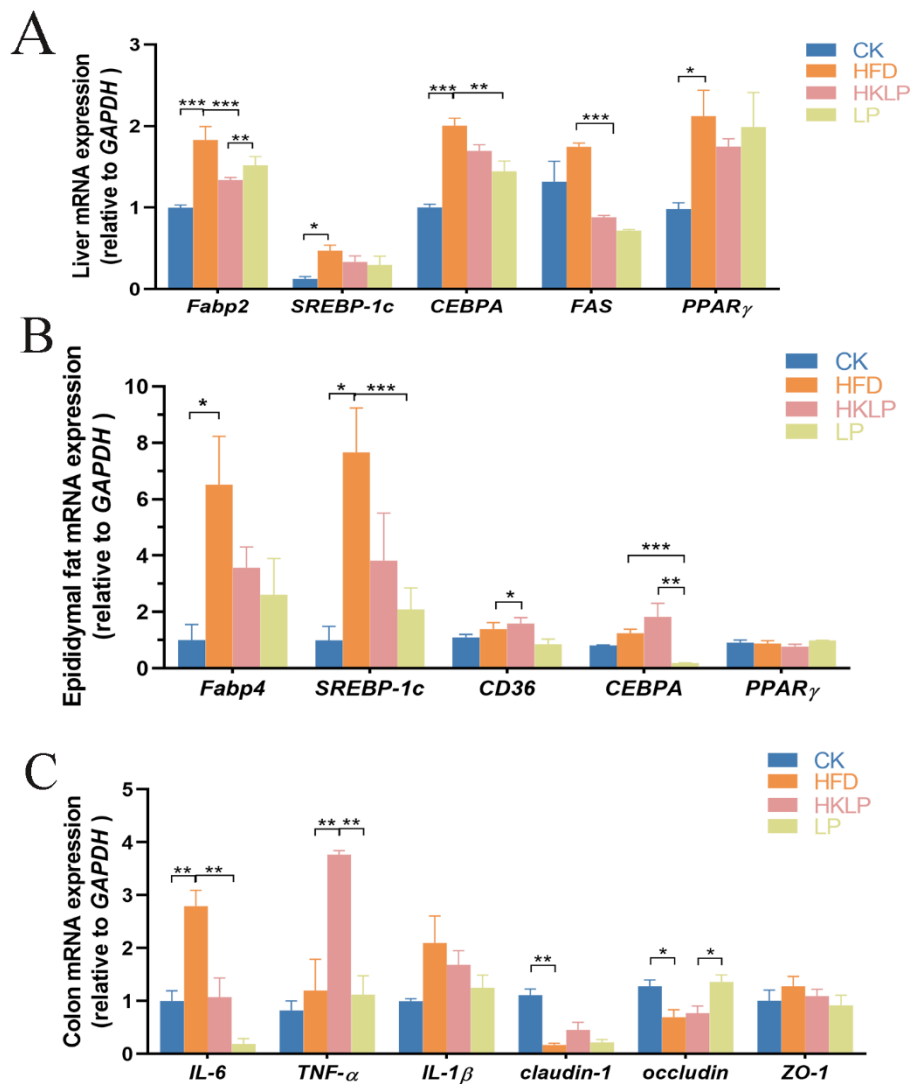


Figure 4 Effects of *L. plantarum* KX041 on transcription levels of inflammatory obesity-related genes in different tissues. (A) expression of related genes in liver tissue (*Fabp2*, *SREBP-1c*, *CEBP*, *FAS*, *PPAR γ*); (B) expression of related genes in epididymal fat (*Fabp4*, *SREBP-1c*, *CD36*, *CEBP*, *PPAR γ*); (C) expression of related genes in colon tissue (*IL-6*, *TNF- α* , *IL-1 β* , *Claudin-1*, *Occludin*, *ZO-1*). *, ** and *** represent $P < 0.05$, 0.01 and 0.001 respectively.

Adipocyte hyperplasia and hypertrophy constitute the fundamental pathological basis of obesity. In adipose tissue (Figure 4B), compared to CK group, the HFD group exhibited significantly elevated gene expression only in *Fabp4* and *SREBP-1c*. Live *L. plantarum* KX041 intervention markedly reduced *SREBP-1c* and *CEBPA* expression levels. These results demonstrate that live *L. plantarum* KX041 exerts inhibitory effects on lipid accumulation in adipose tissue. The differences between live and inactivated bacteria may be attributed to metabolites or extracellular polysaccharides produced by *L. plantarum* KX041.

In prior studies, EPS generated by *L. plantarum* KX041 was used to intervene in pre-adipocytes, and it was found that 400ug/mL of EPS could significantly inhibit the transcriptional level of CEBPA mRNA [10]. Furthermore, emerging evidence indicates that aqueous extracts of *Eucommia ulmoides* effectively downregulate mRNA expression of *SREBP-1c* by modulating gut microbiota composition and key metabolic intermediates such as bilirubin and lithocholic acid, thereby contributing to the regulation of lipid metabolism [33].

Furthermore, obesity may lead to colonic barrier dysfunction and increased intestinal permeability [34]. RT-PCR analysis of intestinal tissue (Figure 4C) revealed that HFD group exhibited significantly elevated *IL-6* gene expression and markedly reduced levels of tight junction proteins (*Claudin-1* and *Occludin*). In contrast, *L. plantarum* KX041 intervention significantly normalized *IL-6* and *Occludin* expression, thereby mitigating gut inflammatory damage.

3.5 *L. Plantarum* KX041 regulates intestinal flora and SCFAs

The gut microbiota is recognized as a "second organ" of the human body. Mounting evidence indicates its association with the development and progression of obesity and related metabolic disorders [35]. Consequently, 16S rRNA gene sequencing was employed to analyze the effects of *L. plantarum* KX041 on gut microbial composition. In α -diversity analysis, four indices—ACE, Chao1, Simpson, and Shannon—were employed to assess microbial community diversity and richness (Figure 5A). The results demonstrated that HFD intervention significantly increased the diversity of gut microbiota in mice, and *L. plantarum* KX041 supplementation further enhanced this effect.

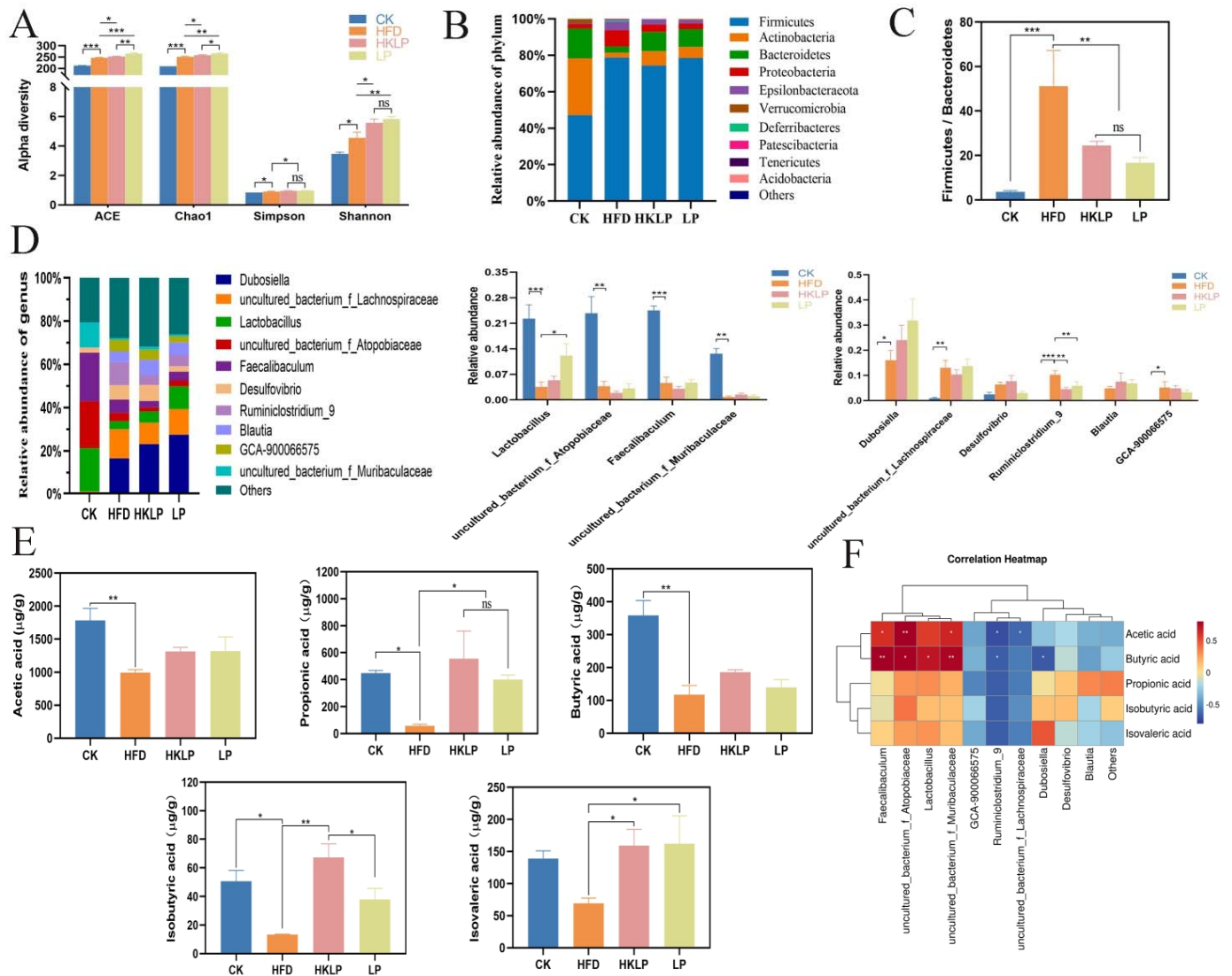


Figure 5 Effect of *L. plantarum* KX041 on gut microbiota composition and SCFAs. (A) Alpha diversity Index; (B) relative abundance of phylum level; (C) Firmicutes/Bacteroidetes abundance; (D) relative abundance at the genus level and significance analysis; (E) the content of SCFAs; (F) the correlation analysis with SCFA and bacterial flora. *, ** and *** represent $P < 0.05$, 0.01 and 0.001 respectively.

Analysis of microbial composition at the phylum and genus levels revealed that HFD significantly altered the gut microbiota profile. At the phylum level, *L. plantarum* KX041 intervention effectively mitigated obesity-induced phylum-level dysbiosis, significantly reducing the elevated F/B ratio (Figure 5B and C). At the genus level, significance analysis of the top 10 most abundant microbes revealed that HFD significantly reduced the abundance of 4 microbial taxa while increasing 4 others (Figure 5D). Notably, obesity led to a marked decrease in *Lactobacillus* abundance, which was significantly restored after intervention with live *L. plantarum* KX041. This may be attributed to the ability of viable *L. plantarum* KX041 to colonize, metabolize, and replicate within the intestinal environment, thereby increasing its abundance through interactions with the host or other bacterial species, such as via cross-feeding mechanisms. For instance, studies have demonstrated that in β -glucan (BG) intervention experiments, *Lactobacillus* exhibits increased abundance through cross-feeding interactions with *Bacteroides hominis* [36]. In contrast, thermally inactivated *Lactobacillus* lose their viability due to heat treatment and are consequently unable to replicate or carry out metabolic activities, which prevents any increase in abundance. Their functional effects rely instead on modulating the host's

immune response—such as activating innate immunity—rather than on microbial proliferation [25]. Recent studies have demonstrated that *Lactobacillus* strains exhibit physiological activities capable of ameliorating obesity and dyslipidemia [37, 38]. Furthermore, obesity significantly increased the abundance of *Ruminiclostridium_9*, which was markedly reduced by both heat-inactivated and live *L. plantarum* KX041 interventions. *Ruminiclostridium_9* is a gut microbiota member whose abundance positively correlates with obesity phenotypes [39]. These findings demonstrate that *L. plantarum* KX041 can ameliorate obesity by modulating the abundances of *Lactobacillus* and *Ruminiclostridium_9*.

The gut microbiota mediates multifaceted beneficial effects on metabolic syndrome through its metabolites, particularly SCFAs), which modulate energy supply, insulin sensitivity, and lipid homeostasis [40]. These microbial-derived compounds directly or indirectly regulate obesity-associated pathophysiological processes [41]. Fecal SCFA analysis revealed that acetate, propionate, and butyrate were the predominant colonic short-chain fatty acid metabolites across all groups, with acetate exhibiting the highest concentration (Figure 5E). The average SCFAs content in HFD was significantly lower than in CK, whereas *L. plantarum* KX041 intervention notably increased the levels of propionate, isobutyrate, and isovalerate. SCFAs contribute to body weight control and lipid homeostasis. For instance, acetate has been demonstrated to activate hypothalamic neurons, thereby suppressing appetite [42], while butyrate serves as the primary energy source for colonocytes, not only ameliorating intestinal inflammation but also preserving epithelial barrier integrity [43]. The increase in SCFAs may be attributed to EPS produced by *L. plantarum* KX041. For instance, studies have shown that elevated abundance of *Bacteroides*—a genus capable of fermenting polysaccharides into propionate and acetate [44].

Correlation analysis revealed that the abundance of *Lactobacillus*, which was significantly enriched after LP intervention, was proportional to the levels of acetic and butyric acids. In addition, studies have also demonstrated that *Lactobacillus* can promote co-enrichment with *Bacteroides* through cross-feeding, and both *Bacteroides* and *Lactobacillus* can produce SCFAs through metabolism [45]. Conversely, the abundance of *Ruminiclostridium_9*, which was significantly reduced by HKLP and LP, was inversely proportional to the levels of acetic and butyric acids (Figure 5F).

This suggests that the intestinal microbiota community structure in mice following intervention with *L. plantarum* KX041 is significantly associated with the levels of SCFAs. Furthermore, existing literature indicates that certain bacterial genera are capable of synthesizing SCFAs. Thus, a potential causal relationship may exist between the gut microbiota and intestinal metabolites (SCFAs), although the underlying mechanisms require further investigation through subsequent experimental studies.

3.6 The application of *L. Plantarum* KX041 in Dairy Products

Both *L. Plantarum* KX041 and the EPS [10] it produces have been demonstrated to possess functional activities in alleviating inflammatory obesity and improving the gut microbiota. Thus, this study further explores the potential of *L. Plantarum* KX041 as an excellent dairy starter culture for dairy product development. Using a commercial fermentation bacteria as the control group, a single strain of *L. Plantarum*

KX041 was inoculated into fresh milk supplemented with 3%, 5%, and 7% (w/v) sucrose for fermentation. The results indicated that the commercial bacteria, composed of five commercial bacteria (*Lactobacillus bulgaricus*, *Streptococcus thermophilus*, *Lactobacillus acidophilus*, *Lactobacillus plantarum*, and *Lactobacillus casei*), coagulated after approximately 6 h of fermentation. In contrast, the single-strain fermentation of *L. Plantarum* KX041 led to coagulation after 12 h (Figure 6A). Moreover, no significant differences in coagulation time were observed among different sucrose addition levels. Through sensory evaluation, it was determined that the yogurt with 7% sucrose addition exhibited the optimal taste, with moderate acidity, a delicate and homogeneous texture, and no whey separation (Figure 6B). Consequently, the pH of the *L. Plantarum* KX041-fermented yogurt with 7% sucrose addition and the commercial bacteria-fermented yogurt were subsequently measured. The findings revealed that within the first 12 h, the pH of the 7% *L. Plantarum* KX041 group rapidly decreased from 6.5 to 4.5. As lactic acid accumulated, the increased acidity promoted the proliferation of *Lactobacillus*, causing the rate of pH decline to slow down. Conversely, for the commercial bacteria group, the pH dropped rapidly from 6.5 to 4.5 within the first 6 h and then remained stable (Figure 6C). This observation was consistent with the yogurt coagulation time.

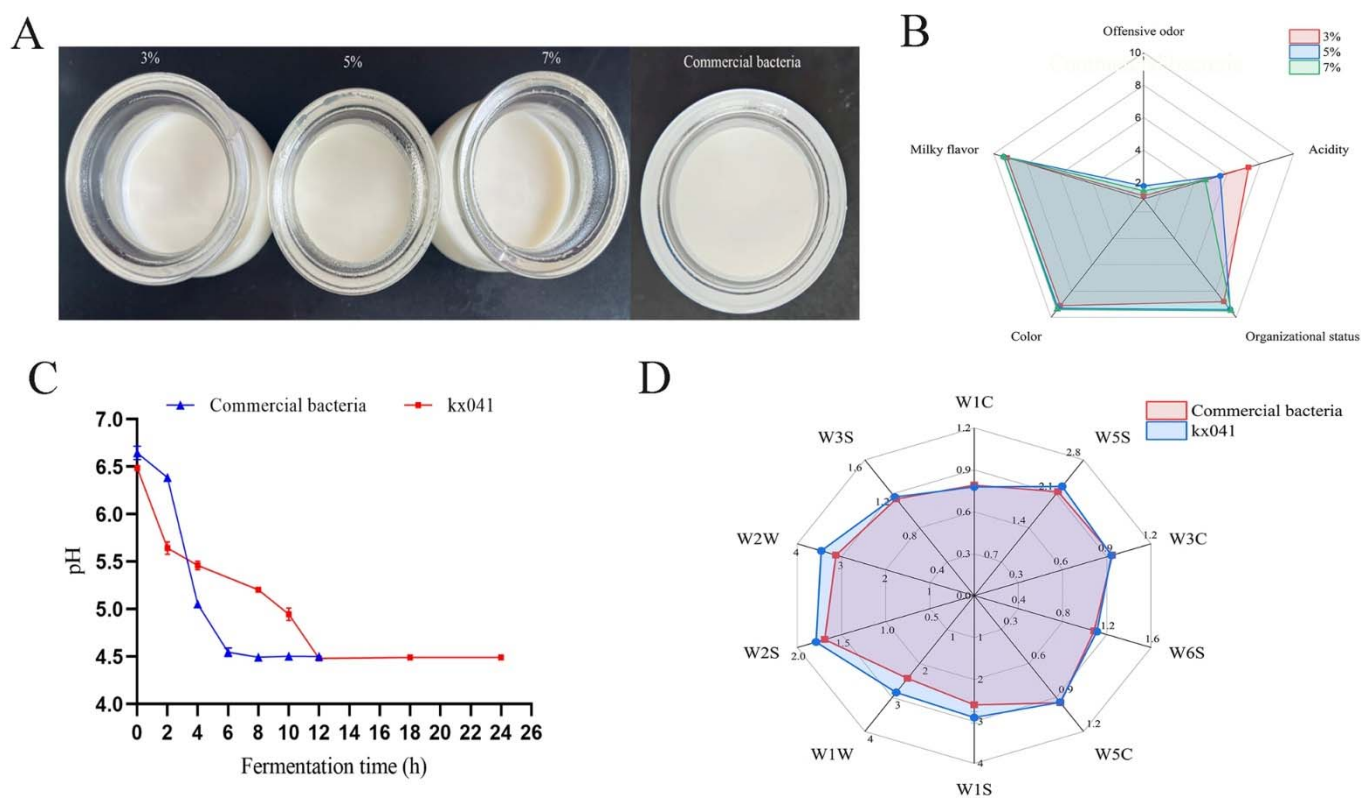


Figure 6 Application of *L. plantarum* KX041 in dairy fermentation. (A) Effects of 3%, 5% and 7% sucrose addition on curd characteristics of *L. plantarum* KX041 single bacterial fermentation; (B) sensory evaluation of fermented yogurt with *L. plantarum* KX041 at different sucrose concentrations (3%, 5% and 7%); (C) pH variation curd during *L. plantarum* KX041 single bacterial fermentation and commercial bacterial fermentation; (D) flavor characteristics of *L. plantarum* KX041 single bacterial fermentation and commercial bacterial fermentation by electron nose detection.

The flavors of commercial bacteria and *L. Plantarum* KX041 single-strain fermented milk were analyzed using an electronic nose (Figure 6D). The study revealed distinct flavor profiles between the two yogurts, particularly in W1W (inorganic sulfur compounds), W2W (aromatic and organic sulfur compounds), and

W2S (alcohols and ketones). Sulfur compounds are generated through the microbial metabolism of sulfur-containing amino acids or the decomposition of sulfo groups during the pre-fermentation heat treatment of yogurt, which accounts for the cooked flavor in heated milk [46]. The production of alcohols and ketone aldehyde may be caused by the production of small amounts of ethanol, propanol, butanol and other alcohols by *Lactobacillus* in the metabolic process, which give yogurt its alcoholic aroma [47]. *L. Plantarum* KX041 may have a stronger ability to decompose sulfur-containing amino acids (such as methionine, cysteine), and a unique oxidation pathway for fatty acids or sugars, thereby generating a richer aromatic odor. Moreover, *L. plantarum* KX041 produces more aromatic alcohols than commercial bacteria. Commercial bacteria fermentation is a mixed strain fermentation, the metabolism of different strains may restrict each other, generating metabolites that inhibit the formation of sulfides [48]. Although the inorganic sulfides produced by single-cell fermentation are slightly more than those produced by mixed bacteria, the sensory evaluation does not affect the taste and flavor. Therefore, based on the functional and fermentation characteristics of *L. Plantarum* KX041, it has the potential to be used as a single-cell fermentation agent to develop functional dairy products. Furthermore, to further enhance the yogurt flavor, it is essential to select probiotics that can consume sulfides with *L. Plantarum* KX041 and conduct mixed bacterial fermentation in the later stage. Meanwhile, since it can produce functional EPS, During the development of dairy products, EPS can also be purified and used as a natural thickener or natural active substance in the development of dairy products.

4. Conclusions

The probiotic potential of *L. plantarum* KX041 is evidenced by its ability to alleviate high-fat diet-induced inflammatory obesity, as well as its favorable characteristics for single-strain fermentation. *L. plantarum* KX041 exerts beneficial effects on inflammatory obesity by modulating key contributing factors, including lipid accumulation, dyslipidemia, hepatic function, and intestinal integrity, along with restoring the balance of gut microbiota and SCFAs. Furthermore, *L. plantarum* KX041 exhibits strong fermentation performance, enabling the production of yogurt with a characteristic aroma and milk flavor comparable to those obtained using commercial strains. Therefore, *L. Plantarum* KX041 may have great potential as a new ingredient for the development of functional dairy products.

Declaration of competing interest

There are no potential conflicts of interest to report.

Acknowledgment

The author thanks the financial support of National Natural Science Foundation of China (Grant No. 32401999), Shaanxi Science and Technology Innovation Team Project (2024RS-CXTD-75), Central Government Funds to Guide Local Science and Technology Development (2024ZY-JCYJ-02-45), Shaanxi Key R&D Plan Project - Key Industrial Innovation Chain Project (2023-ZDLNY-35, 2024NC-ZDCYL-03-10).

Reference

- [1] M.A. Abbas, N. Bobby, E.B. Lee, J.H. Hong, S.C. Park, Anti-Obesity Effects of *Ecklonia cava* Extract in High-Fat Diet-Induced Obese Rats, *Antioxidants* 11 (2) (2022), <https://doi.org/10.3390/antiox11020310>.
- [2] L. Turner, A.I. Wanasinghe, P. Brunori, S. Santosa, Is Adipose Tissue Inflammation the Culprit of Obesity-Associated Comorbidities?, *Obes. Rev.* (2025), <https://doi.org/10.1111/obr.13956>.
- [3] T.V. Rohm, D.T. Meier, J.M. Olefsky, M.Y. Donath, Inflammation in obesity, diabetes, and related disorders, *Immunity* 55 (1) (2022) 31-55, <https://doi.org/10.1016/j.immuni.2021.12.013>.
- [4] H.X. Zhu, X.H. Yi, M.Y. He, S.Y. Wu, M. Li, S. Gao, Exploring the interplay of genetic variants and environmental factors in childhood obesity: A systematic review and meta-analysis, *Metab Clin Exp* 170 (2025), <https://doi.org/10.1016/j.metabol.2025.156303>.
- [5] M. Régnier, M. Van Hul, M. Roumain, A. Paquot, A.D. d'Oplinter, F. Suriano, A. Everard, N.M. Delzenne, G.G. Muccioli, P.D. Cani, Inulin increases the beneficial effects of rhubarb supplementation on high-fat high-sugar diet-induced metabolic disorders in mice: impact on energy expenditure, brown adipose tissue activity, and microbiota, *Gut Microbes* 15 (1) (2023), <https://doi.org/10.1080/19490976.2023.2178796>.
- [6] Z.T. Lu, Y. Zheng, J. Zheng, Q.J. Liang, Q.C. Zhen, M.J. Cui, H.R. Yang, H.T. Wu, C.X. Tian, K.M. Zhu, C.Y. Bian, L. Du, H. Wu, X. Guo, Theabrownin from Fu Brick tea ameliorates high-fat induced insulin resistance, hepatic steatosis, and inflammation in mice by altering the composition and metabolites of gut microbiota, *Food Funct.* 15 (8) (2024) 4421-4435, <https://doi.org/10.1039/d3fo05459d>.
- [7] Y.C. Lin, Y.T. Chen, K.Y. Li, M.J. Chen, Investigating the Mechanistic Differences of Obesity-Inducing *Lactobacillus kefiranofaciens* M1 and Anti-obesity *Lactobacillus mali* APS1 by Microbolomics and Metabolomics, *Front Microbiol* 11 (2020) 1454, <https://doi.org/10.3389/fmicb.2020.01454>.
- [8] B.L. Wei, Z. Peng, M.Y. Xiao, T. Huang, W.D. Zheng, M.Y. Xie, T. Xiong, Three lactic acid bacteria with anti-obesity properties: In vitro screening and probiotic assessment, *Food Biosci* 47 (2022), <https://doi.org/ARTN10172410.1016/j.fbio.2022.101724>.
- [9] D. Kim, Y. Choi, S. Kim, J. Ha, H. Oh, Y. Lee, Y. Kim, Y. Seo, E. Park, J. Kang, Y. Yoo, S. Lee, H. Lee, Y. Yoon, *Lactobacillus fermentum* SMFM2017-NK4 Isolated from Kimchi Can Prevent Obesity by Inhibiting Fat Accumulation, *Foods* 10 (4) (2021), <https://doi.org/10.3390/foods10040772>.
- [10] F.F. Yue, H.Y. Han, J.X. Xu, X.Y. Yao, Y.T. Qin, L.B. Zhang, X. Sun, J.H. Huang, F. Zhang, X. Lü, Effects of exopolysaccharides from *Lactobacillus plantarum* KX041 on high fat diet-induced gut microbiota and inflammatory obesity, *Int. J. Biol. Macromol.* 289 (2025), <https://doi.org/10.1016/j.ijbiomac.2024.138803>.
- [11] D.-W. Zheng, R.-Q. Li, J.-X. An, T.-Q. Xie, Z.-Y. Han, R. Xu, Y. Fang, X.-Z. Zhang, Prebiotics-Encapsulated Probiotic Spores Regulate Gut Microbiota and Suppress Colon Cancer, *Adv. Mater.* 32 (45) (2020), <https://doi.org/10.1002/adma.202004529>.
- [12] S.Y. Song, A. Jeong, J. Lim, B.K. Kim, D.J. Park, S. Oh, *Lactiplantibacillus plantarum* L67 probiotics vs paraprobiotics for reducing pro-inflammatory responses in colitis mice, *Int J Dairy Technol* (2022), <https://doi.org/10.1111/1471-0307.12918>.
- [13] Y.M. Xu, Y.L. Cui, X. Wang, F.F. Yue, Y.Y. Shan, B.F. Liu, Y. Zhou, Y.L. Yi, X. Lu, Purification, characterization and bioactivity of exopolysaccharides produced by *Lactobacillus plantarum* KX041, *Int. J. Biol. Macromol.* 128 (2019) 480-492, <https://doi.org/10.1016/j.ijbiomac.2019.01.117>.
- [14] J.Y. Eor, M.-J. Kwak, M.Y. Park, S.-w. Choi, K.-Y. Whang, Y. Kim, Anti-obesity effect of seaweed algae (*Ascophyllum nodosum*) extracts in the 3T3-L1 cell line and a high-fat diet-induced obesity rat model, *Food Biosci* 59 (2024), <https://doi.org/10.1016/j.fbio.2024.104176>.
- [15] L. Li, J.R. Lin, C.H. Huang, J.M. Liu, Y. Yuan, Z.X. Liu, Y.Y. Li, W. Li, A.P. Diao, The TFEB activator clomiphene citrate ameliorates lipid metabolic syndrome pathology by activating lipophagy and lipolysis, *Biochem. Pharmacol.* 232 (2025), <https://doi.org/10.1016/j.bcp.2024.116694>.

- [16] M.M. Vazquez, M.V. Gutierrez, S.R. Salvatore, M. Puiatti, V.A. Dato, G.A. Chiabrando, B.A. Freeman, F.J. Schopfer, G. Bonacci, Nitro-oleic acid, a ligand of CD36, reduces cholesterol accumulation by modulating oxidized-LDL uptake and cholesterol efflux in RAW264.7 macrophages, *Redox Biology* 36 (2020), <https://doi.org/10.1016/j.redox.2020.101591>.
- [17] Z.Y. Song, A.M. Xiaoli, Q.W. Zhang, Y. Zhang, E.S.T. Yang, S. Wang, R. Chang, Z.D.D. Zhang, G.S. Yang, R. Strich, J.E. Pessin, F.J. Yang, Cyclin C regulates adipogenesis by stimulating transcriptional activity of CCAAT/enhancer-binding protein α , *J. Biol. Chem.* 292 (21) (2017) 8918-8932, <https://doi.org/10.1074/jbc.M117.776229>.
- [18] X. Li, H.H. Yu, R.X. Tian, X.X. Wang, T. Xing, C.Y. Xu, T.T. Li, X. Du, Q.Q. Cui, B. Yu, Y.X. Cao, Z.Z. Yin, FABP4 as a Mediator of Lipid Metabolism and Pregnant Uterine Dysfunction in Obesity, *Adv. Sci* (2025), <https://doi.org/10.1002/advs.202501077>.
- [19] V. Wayal, C.C. Hsieh, Bioactive dipeptides mitigate high-fat and high-fructose corn syrup diet-induced metabolic-associated fatty liver disease via upregulation of Nrf2/HO-1 expressions in C57BL/6J mice, *Biomed. Pharmacother.* 168 (2023), <https://doi.org/10.1016/j.biopha.2023.115724>.
- [20] E. Lee, H. Korf, A. Vidal-Puig, An adipocentric perspective on the development and progression of non-alcoholic fatty liver disease, *J. Hepatol.* 78 (5) (2023) 1048-1062, <https://doi.org/10.1016/j.jhep.2023.01.024>.
- [21] S. Das, D. Choudhuri, Dietary calcium regulates the insulin sensitivity by altering the adipokine secretion in high fat diet induced obese rats, *Life Sci.* 250 (2020), <https://doi.org/10.1016/j.lfs.2020.117560>.
- [22] J. Santos, J.M. La Fuente, A. Fernández, P. Ruano, J. Angulo, LDL-c/HDL-c Ratio and NADPH-Oxidase-2-Derived Oxidative Stress as Main Determinants of Microvascular Endothelial Function in Morbidly Obese Subjects, *Antioxidants* 13 (9) (2024), <https://doi.org/10.3390/antiox13091139>.
- [23] C.L. Kuo, B. Ting, R.J.H. Tseng, S.P. Liu, J.Y. Liou, Comparative Efficacy of *Antrodia cinnamomea* on Liver Function Biomarkers in Mice and Rats: A Network Meta-Analysis, *Antioxidants* 14 (6) (2025), <https://doi.org/10.3390/antiox14060660>.
- [24] Y. Wu, D.J. Gao, Y.J. Pan, Y. Dong, Z.Y. Bai, S.B. Gu, Modulation of Serum Metabolic Profiles by *Bifidobacterium breve* BBr60 in Obesity: A Randomized Controlled Trial, *Foods* 13 (22) (2024), <https://doi.org/10.3390/foods13223655>.
- [25] X.H. Wu, D.H. Yu, Y.K. Ma, X.X. Fang, P.D. Sun, Function and therapeutic potential of Amuc_1100, an outer membrane protein of *Akkermansia muciniphila*: A review, *Int. J. Biol. Macromol.* 308 (2025), <https://doi.org/10.1016/j.ijbiomac.2025.142442>.
- [26] L. Boutens, G.J. Hooiveld, S. Dhingra, R.A. Cramer, M.G. Netea, R. Stienstra, Unique metabolic activation of adipose tissue macrophages in obesity promotes inflammatory responses, *Diabetologia* 61 (4) (2018) 942-953, <https://doi.org/10.1007/s00125-017-4526-6>.
- [27] C.O. Marginean, L.E. Melit, A. Hutanu, D.V. Ghiga, M.O. Sasaran, The adipokines and inflammatory status in the era of pediatric obesity, *Cytokine* 126 (2020), <https://doi.org/10.1016/j.cyto.2019.154925>.
- [28] H.Y. Xu, G.T. Barnes, Q. Yang, Q. Tan, D.S. Yang, C.J. Chou, J. Sole, A. Nichols, J.S. Ross, L.A. Tartaglia, H. Chen, Chronic inflammation in fat plays a crucial role in the development of obesity-related insulin resistance, *J. Clin. Investig.* 112 (12) (2003) 1821-1830, <https://doi.org/10.1172/jci200319451>.
- [29] Y.Q. Cao, Y.Y. Chen, K. Miao, S.Y. Zhang, F.C. Deng, M. Zhu, C. Wang, W. Gu, Y.X. Huang, Z.J. Shao, X.Y. Dong, Y.F. Gong, H. Peng, H. Yang, Y. Wan, X.D. Jia, S. Tang, PPAR γ As a Potential Target for Adipogenesis Induced by Fine Particulate Matter in 3T3-L1 Preadipocytes, *Environ. Sci. Technol.* 57 (20) (2023) 7684-7697, <https://doi.org/10.1021/acs.est.2c09361>.
- [30] S. Satoh, D. Onomura, Y. Ueda, H. Dansako, M. Honda, S. Kaneko, N. Kato, Ribavirin-induced down-regulation of CCAAT/enhancer-binding protein α leads to suppression of lipogenesis, *Biochem. J.* 476 (2019) 137-149, <https://doi.org/10.1042/bcj20180680>.
- [31] X. Huang, Y.C. Zhou, Y.W. Sun, Q.J. Wang, Intestinal fatty acid binding protein: A rising therapeutic target in lipid metabolism, *Prog. Lipid Res.* 87 (2022), <https://doi.org/10.1016/j.plipres.2022.101178>.
- [32] S. Bae, I. Ullah, J. Beloor, J. Lim, K. Chung, Y. Yi, E. Kang, G. Yun, T. Rhim, S.-K. Lee, Blocking Fas-signaling in adipocytes and hepatocytes prevents obesity-associated inflammation, insulin resistance, and hepatosteatosis, *J Ind Eng Chem* 135 (2024) 434-443, <https://doi.org/https://doi.org/10.1016/j.jiec.2024.01.055>.

- [33] Y. Duan, F.Q. Guo, C. Li, D.H. Xiang, M. Gong, H. Yi, L.M. Chen, L.H. Yan, D. Zhang, L.P. Dai, X.Q. Liu, Z.M. Wang, Aqueous extract of fermented *Eucommia ulmoides* leaves alleviates hyperlipidemia by maintaining gut homeostasis and modulating metabolism in high-fat diet fed rats, *Phytomedicine* 128 (2024), <https://doi.org/10.1016/j.phymed.2023.155291>.
- [34] Q. Nie, Y. Sun, W. Hu, C. Chen, Q. Lin, S. Nie, Glucmannan promotes *Bacteroides ovatus* to improve intestinal barrier function and ameliorate insulin resistance, *Imeta* 3 (1) (2024), <https://doi.org/10.1002/imt2.163>.
- [35] K. Wang, X.Y. Liang, Y.L. Pang, C.T. Jiang, The Role of Gut Microbiota in Host Lipid Metabolism: An Eye on Causation and Connection, *Small Methods* 4 (7) (2020), <https://doi.org/10.1002/smt201900604>.
- [36] S.S. Zhang, Q.X. Nie, Y.G. Sun, S. Zuo, C.H. Chen, S. Li, J.R. Yang, J.L. Hu, X.T. Zhou, Y.K. Yu, P. Huang, L. Lian, M.Y. Xie, S.P. Nie, *Bacteroides uniformis* degrades β -glucan to promote *Lactobacillus johnsonii* improving indole-3-lactic acid levels in alleviating colitis, *Microbiome* 12 (1) (2024), <https://doi.org/10.1186/s40168-024-01896-9>.
- [37] B.L. Wei, Z. Peng, M.Y. Xiao, T. Huang, W.D. Zheng, M.Y. Xie, T. Xiong, Three lactic acid bacteria with anti-obesity properties: *In vitro* screening and probiotic assessment, *Food Biosci* 47 (2022), <https://doi.org/10.1016/j.fbio.2022.101724>.
- [38] J. Minj, P. Chandra, C. Paul, R.K. Sharma, Bio-functional properties of probiotic *Lactobacillus*: current applications and research perspectives, *Crit. Rev. Food Sci. Nutr.* 61 (13) (2021) 2207-2224, <https://doi.org/10.1080/10408398.2020.1774496>.
- [39] Y. Lan, L.L. Chang, J. Peng, M.Q. Zhang, Q.Y. Sun, R.X. Qiao, X.L. Hou, X.C. Ding, Q. Zhang, Q. Peng, J.E. Dong, X.B. Liu, Z.Y. Ma, Sea buckthorn polysaccharide ameliorates high-fat diet induced mice neuroinflammation and synaptic dysfunction via regulating gut dysbiosis, *Int. J. Biol. Macromol.* 236 (2023), <https://doi.org/10.1016/j.ijbiomac.2023.123797>.
- [40] F. Ahmad, P. Saha, V. Singh, M. Wahid, R.K. Mandal, B.N. Mishra, S. Fagoonee, S. Haque, Diet as a modifiable factor in tumorigenesis: Focus on microbiome-derived bile acid metabolites and short-chain fatty acids, *Food Chem.* 410 (2023), <https://doi.org/10.1016/j.foodchem.2022.135320>.
- [41] P.L. de Freitas, M.V.C. Barros, R. Frões, L.M. França, A.M.D. Paes, Prebiotic effects of plant-derived (poly)phenols on host metabolism: Is there a role for short-chain fatty acids?, *Crit. Rev. Food Sci. Nutr.* 63 (33) (2023) 12285-12293, <https://doi.org/10.1080/10408398.2022.2100315>.
- [42] N. Forte, B. Marfella, A. Nicois, L. Palomba, D. Paris, A. Motta, M.P. Mollica, V. Di Marzo, L. Cristino, The short-chain fatty acid acetate modulates orexin/hypocretin neurons: A novel mechanism in gut-brain axis regulation of energy homeostasis and feeding, *Biochem. Pharmacol.* 226 (2024), <https://doi.org/10.1016/j.bcp.2024.116383>.
- [43] S.S. Miao, J.K. Li, Y. Chen, W.Y. Zhao, M.R. Xu, F. Liu, X.T. Zou, X.Y. Dong, Targeting gut microbiota and metabolism profiles with coated sodium butyrate to ameliorate high-energy and low-protein diet-induced intestinal barrier dysfunction in laying hens, *Anim. Nutr* 19 (2024) 104-116, <https://doi.org/10.1016/j.aninu.2024.06.006>.
- [44] K. Ye, C.J. Fu, S. Ma, H.J. Du, S.G. Chen, D.H. Liu, G.X. Ma, H. Xiao, Comprehensive assessment of *Hypsizygus marmoreus* polysaccharides through simulated digestion and gut microbiota fermentation *in vitro*, *Food Hydrocolloids* 144 (2023), <https://doi.org/10.1016/j.foodhyd.2023.108989>.
- [45] S.C. Tian, Y.T. Lei, F.L. Zhao, J.W. Che, Y.H. Wu, P. Lei, Y.E. Kang, Y.J. Shan, Improving insulin resistance by sulforaphane via activating the *Bacteroides* and *Lactobacillus* SCFAs-GPR-GLP1 signal axis, *Food Funct.* 15 (17) (2024), <https://doi.org/10.1039/d4fo01059k>.
- [46] J. Pereda, D.P. Jaramillo, J.M. Quevedo, V. Ferragut, B. Guamis, A.J. Trujillo, Characterization of volatile compounds in ultra-high-pressure homogenized milk, *Int. Dairy J* 18 (8) (2008) 826-834, <https://doi.org/10.1016/j.idairyj.2007.12.002>.
- [47] N.Y. Liang, Z. Zhao, J.M. Curtis, M.G. Gänzle, Antifungal cultures and metabolites of lactic acid bacteria for use in dairy fermentations, *Int. J. Food Microbiol.* 383 (2022), <https://doi.org/10.1016/j.ijfoodmicro.2022.109938>.
- [48] L. Zhao, R. Feng, F. Ren, X. Mao, Addition of buttermilk improves the flavor and volatile compound profiles of low-fat yogurt, *LWT* 98 (2018) 9-17, <https://doi.org/10.1016/j.lwt.2018.08.029>.